












Characteristics of fast deuteron sources generated in a dense plasma focus

P. Kubes^{1,a} , M. Paduch², M. J. Sadowski³ , J. Cikhardt¹ , B. Cikhardtova¹ ,
D. Klir¹ , J. Kravarik¹, R. Kwiatkowski³ , V. Munzar¹, K. Rezac¹ ,
A. Szymaszek², K. Tomaszewski² , D. Zaloga³, E. Zielinska², M. Akel⁴ 

¹ Czech Technical University in Prague, 166-27 Prague, Czech Republic

² Institute of Plasma Physics and Laser Microfusion, 01-497 Warsaw, Poland

³ National Centre for Nuclear Research, 05-400 Otwock-Świerk, Poland

⁴ Department of Physics, Atomic Energy Commission, P.O. Box 6091, Damascus, Syria

Received: 8 December 2020 / Accepted: 24 July 2021

© The Author(s), under exclusive licence to Società Italiana di Fisica and Springer-Verlag GmbH Germany, part of Springer Nature 2021

Abstract The paper characterizes sources of the fast deuterons which can produce the D–D fusion neutrons. Two pinhole cameras, the axial one and the slant one (oriented at 0° and 60° in relation to the z-axis), were equipped with solid-state nuclear track detectors and applied to investigate the fast deuterons of energies about 100 keV, which produce small quasi-circular track spots of diameters ranging (1–3) mm. They are often observed in plasma-focus shots with higher neutron yields, when they constitute a part of the recorded ion images in a form of azimuthal arcs and/or radial strips. An analysis of an influence of the global magnetic field, which acts along the fast deuteron trajectories, made it possible to determinate the deuteron sources localization, also outside the dense plasma column. The recorded spatial distribution of the fast deuterons, their temporal correlation with disruptions of the ordered plasma structures inside and outside the pinch column, and a regular evolution of the energy of fast deuterons—indicate their strong interconnection and the link with filamentary structure of the current flow.

1 Introduction

The fast electrons and ions of energies ranging tens and hundreds keV are often emitted from magnetized plasmas produced in laboratories and space. Their effective nonthermal acceleration mechanism is under intensive studies. A magnetic reconnection, considered as one of the possible acceleration models, assumes a release of the magnetic energy during transformation of the ordered plasma structures, which can be formed by the closed currents and their magnetic fields. This possibility has been described in detail in a paper [1], which summarized the results of experiments and numerical simulations performed for tokamaks, reverse pinches, magnetosphere, and solar-flare plasmas. This paper mentioned also temporal correlations of the observed individual (relatively small) sources of the fast particles with transformations of the larger ordered plasma structures in magnetized plasma of a lower

^a e-mail: kubes@fel.cvut.cz (corresponding author)

density. The model of the magnetic reconnection has also been applied for denser plasmas produced by the interaction of focused laser beams with some targets [2, 3], when the internal current jets and magnetic fields can evolve and become self-organized. In Z-pinch and dense plasma-focus (PF) experiments, the problem of the fast particle acceleration has been studied and discussed for a long time, in many papers [4–13]. At the deuterium gas filling the accelerated fast deuterons can produce fusion neutrons by a beam-target mechanism.

Numerous PF discharges with the deuterium filling, which were devoted to the studies of plasma transformations and fusion neutrons production, have been studied within a PF-1000 mega-ampere facility at the IPPLM in Warsaw, Poland, during the recent decade [14–20]. Space- and time-resolved measurements with a laser interferometer showed the appearance and evolution of various toroidal and plasmoidal structures. Plasmoids had a spherical-like shape with the maximum density in their centers, while a toroidal-like forms had the maximum density at their internal toroidal axes. These formations were explained by closed currents (with poloidal- and toroidal-components) flowing inside and outside the dense pinch column. The appearance of the closed currents was deduced (on the one hand) from measurements performed with magnetic probes, which showed the existence of a self-generated axial component of the local magnetic field [21, 22]. On the other hand, the knowledge of the plasma density distribution and local temperatures (at the assumption of the quasi-stationary conditions) made it possible to estimate the plasma pressure gradient, which can be explained by a distribution of the force density ($j \times B$) and consequently by the distribution of the currents and their magnetic fields [17, 20]. The closed currents and associated magnetic fields are generated at transformations of a portion of the kinetic energy of the pinched current sheath by a magnetic dynamo effect. This evolution produces the magnetic turbulences, and it leads to the formation of larger ordered structures [23]. They are initially toroidal ones with the dominant toroidal current and poloidal magnetic field, which later on are transformed into a plasmoid of a spheromak-like configuration of the local magnetic field [17, 20]. Their internal high pressure, at the electron temperature of (50–70) eV and a plasma density of $(10^{24}–10^{25}) \text{ m}^{-3}$, can be balanced by the pinching pressure of the discharge current. The magnetic energy confined in the dense column and in its surrounding can be released during disruptions in a form of the kinetic energy of the fast electrons and ions, which are accelerated by strong local electric fields induced by a decay of magnetic fields during magnetic reconnections [15, 18]. A paper published recently [24] has supported theoretically a hypothesis about the crucial role of spontaneously self-organized structures for the fusion neutron emission. It has also presented a qualitative model leading to a description of the magnetic fields associated with such plasma structures.

Sources of the fast deuterons emitted from PF discharges have been studied in many laboratories since the 1960s of the last century. Numerous experimental results, which were summarized, e.g., in papers [4, 25], have stated that the fast deuterons were accelerated in the submillimeter (point-like) sources in a form of narrow microbeams lasting a few ns. The kinetic energy of those deuterons ranged up hundreds keV, and the total energy of the deuteron beams reached a kJ level. The considered sources formed a concentric and/or radial complex image composed of numerous spots of dimensions ranging up to 0.5 mm. A similar circular and radial distribution of the sources emitting MeV-deuterons was also observed in a mega-ampere gas-puffed z-pinch experiment [13]. The acceleration of the deuterons to energy > 20 MeV was explained by a plasma diode mechanism at an increase in the z-pinch impedance ($> 10 \Omega$) during a sub-nanosecond time. A detailed overview of various theoretical explanations has been presented in a paper [7], with a conclusion that the origin of the ion and electron beam acceleration is still controversial. The fast ion beams were investigated also within the PF-1000 facility by means of the ion pinhole cameras equipped

with solid-state nuclear track detectors, as described in two recently published papers [26, 27]. As probable sources of the fast deuterons there were identified two regions: the internal plasmoidal structures and ring-shaped regions in their surroundings, which had diameters ranging even to 15 cm, i.e., considerably larger than the dense pinch column diameter (equal to about 1 cm). The circular sources outside the dense pinch column were described as the layers of two countercurrents composed of the external current (of the value and orientation of the main discharge current) and of the internal closed current flowing partially upon the surface of the dense column. Their magnetic energy transported the pinching pressure from the external regions to the internal plasma structures [28].

The discharge current does not have to be distributed in plasma continuously. The visible and XUV frames showed some filaments, as described in several papers [25, 29–32]. The current origin of these filamentary structures was discussed in other papers [7, 25, 33]. The observed filaments had the radial and azimuthal orientations, the relative long lifetime amounted to tens nanoseconds, and their high energy density could correspond with the production of fast energy particles.

To obtain a more detailed information about characteristics of the deuteron sources, we performed a series of experiments with a new measuring setup which made it possible to improve the spatial resolution of the recorded deuteron tracks from 1 cm, as described in a paper [27], to about 1 mm. The obtained results supported a stronger spatial and temporal correlation of the deuteron sources with a decay of the ordered plasma structures and their filamentary composition.

The experimental facility and diagnostic techniques, which were used in the reported experiments, are described in Sect. 2. Section 3 presents examples of the typical deuteron tracks (recorded by means of the applied pinhole cameras and nuclear track detectors), some conclusions concerning the positions, dimensions, shapes, and mutual connections of the fast deuteron sources, as well as the appearance of an interesting burst of nonthermal soft X-rays. Section 4 presents the summary and conclusions.

2 Description of the device and diagnostics

The experiments described in this paper were performed within the PF-1000 facility (at the IPPLM in Warsaw, Poland), which was equipped with Mather-type coaxial electrodes of 480 mm in length, oriented along the horizontal axis. The anode was made of a copper tube of 230 mm in diameter. The cathode consisted of 12 stainless steel tubes (each of 8 cm in diameter), distributed symmetrically on a 40-cm-dia. cylindrical surface. The filling pressure of pure deuterium was (80–100) Pa. The performed discharges were supplied from a capacitor bank charged up to 16 kV, which stored energy equal to about 250 kJ. The current intensity during the D–D fusion neutron emission amounted to (0.7–0.9) MA. The formation of the pinched plasma column and a higher neutron yield were influenced by a conical tip placed upon the anode front plate. That tip had a shape of the truncated cone with the base of 10 cm in diameter, the height of 2.4 cm, and a central hole of 2 cm in diameter and 2 cm in depth [34].

A setup of the diagnostic equipment, which was applied during the reported experiments, is presented in Fig. 1.

Voltage and current derivative waveforms, as well as the total current intensity values, were measured at the main current collector. Three scintillation detectors (1), coupled with fast photomultipliers, were placed at distances of 7 m from the pinch center, in different directions to the z -axis: downstream (at 0°), upstream (at 180°), and side-on (at 90°). They were used

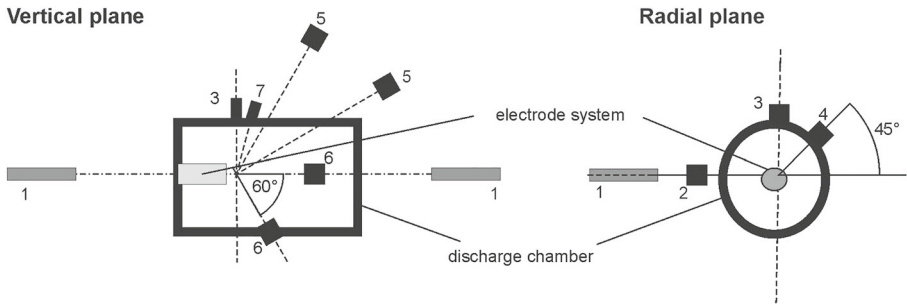


Fig. 1 Scheme of the diagnostics arrangement: 1—scintillation detectors, 2—films recording the interferometric frames, 3—PIN detector of X-rays, 4—soft X-ray framing camera, 5—Ag-activation detectors of fusion neutrons, 6—ion pinhole cameras, 7—X-ray pinhole camera

to determine instants of the emission of hard X-rays (HXR are produced by fast electrons during their collisions with the electrodes and chamber walls [17]) and fusion-produced neutrons and to estimate a mean energy of these neutrons (and the primary deuterons) by means of a time-of-flight method, as described in a paper [35]. The HXRs were filtered by the stainless steel wall of the experimental chamber, which was (1–2) cm in thickness and absorbed radiation up to 100 keV. A Mach–Zehnder interferometer (2), equipped with a diagnostic laser operated at $\lambda = 527$ nm, recorded 15 frames from each plasma discharge, during a period of 210 ns [36]. The interferometer arrangement of parallel half-transmitted mirrors made it possible to observe the interferometric fringes of 1 cm in width for plasma of the electron density equal to about 10^{23} m^{-3} , what determined the boundary uncertainty during the performed measurements. The Abel transformation of the recorded fringes, at the assumption of the cylindrical symmetry, showed that the high-density fringes corresponded to regions with a gradient of the electron concentration, and the dense closed fringes indicated its extremes. Time-resolved soft X-ray (SXR) signals, as obtained from the PIN silicon-detector, shielded with a Be-filter of $10 \mu\text{m}$ in thickness (3), corresponded to photons of energies above 0.7 keV. High-energy ultraviolet (XUV) photons were recorded by means of a four-frame system equipped with pinholes and a micro-channel plate (4). The total neutron yield was measured with two calibrated Ag-activation counters located at different positions (5). In order to record a spatial distribution of the fast deuterons escaping from the PF plasma, the use was made of two ion pinhole cameras (6), which were placed inside the discharge chamber at angles 0° (axial) and 60° (slant) to the z -axis. Those cameras were equipped with solid-state nuclear track detectors of the PM-355 type. Those detectors, applied for deuteron measurements without any absorption filter, had the lower energy threshold equal to about 30 keV. The applied cameras had the inlet diaphragms of $200 \mu\text{m}$ in diameter, which were placed at distance of 30 cm from the anode end. They recorded ion images with the magnification equal to 0.33 and with the uncertainty in the determination of the real objects equal to about 1 mm. The maximum of the current derivative dip was assigned as the $t = 0$ instant. An uncertainty in the timing of different waveforms (recorded during a single discharge) amounted to (3–5) ns.

The energy calibration of the applied nuclear-track detectors of the CR-355 type was performed in the collaboration with an NCBJ-team in Swierk, Poland [37]. In general, the final diameters of the recorded deuteron tracks depend on deuterons energies and the etching conditions. The diameters of the tracks, which were recorded behind absorption Al-filters of different thicknesses, showed a general trend: the higher deuteron energy—the smaller

track diameter and the darker color of the obtained tracks. During the reported experiments, the irradiated CR-355 detectors were etched for 2 h in a 25% water solution of NaOH, at a temperature equal to 70 °C. After etching the tracks of deuterons of energy below 100 keV reached diameters of (3–4) μm and a bright-gray tinge, while those of deuterons of energy above 150 keV had diameters below (2–3) μm and the black color. To analyze the recorded space-resolved tracks of the fast deuterons, we compared them with the time-resolved signals of the fusion-produced neutrons and corresponding interferometric and XUV frames.

3 Experimental results

The described experiments provided new data which delivered more information about sources of the fast deuterons and their interconnection described in our previous papers [26, 27]. It was possible due to the use of the pinhole cameras with a smaller pinhole diameter (decreased from 500 to 200 μm) and the reduction of their distance to the anode end (from 70 to 30 cm). Those changes made it possible to decrease the uncertainty in the determination of deuteron sources from 1 cm to 1 mm. For a detailed analysis of the performed PF-1000 experiments, we have chosen two characteristic shots with relatively high neutron yields above 5×10^{10} : shot #12760 which produced several separated spots of the deuteron tracks in the axial camera image and shot #12759 which produced concentric rings of such tracks. The results obtained from shot #12760 are presented in Figs. 2, 3, 4, and 5, while those from shot #12759 are shown in Figs. 6, 7, and 8.

The characteristic waveforms from shot #12760 with total neutron yield 1×10^{11} are presented in Fig. 2.

A temporal correlation of SXR, HXR, and neutron pulses is shown in Fig. 2a, while Fig. 2b presents similarity and differences of the HXR and neutron pulses recorded by three scintillation detectors placed at different directions. The HXR amplitude was smaller than the neutron pulse amplitude. The neutron signals shown in Fig. 2b have slightly different profiles, which are typical for the dominant neutron pulses observed in all discharges performed within the PF-1000 facility. The neutron signal recorded downstream (blue) shows a sharp rise and slow fall, the side-on signal (green) shows slightly slower rise and fall, while the upstream signal (red) shows a slow rise and fast fall. It can be interpreted by some temporal increase in

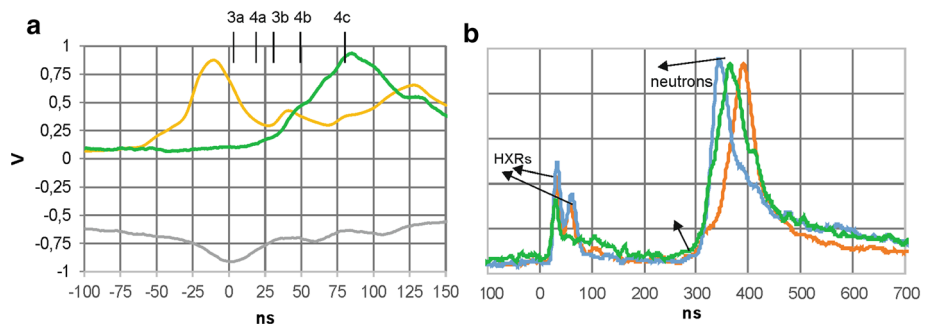


Fig. 2 Data from shot #12760: **a** Waveforms of the current derivative (gray), SXR (yellow), and fusion-produced neutrons (dark green), recorded side-on and shifted back using the time-of-flight method for neutrons of an average energy equal to 2.45 MeV. The marks of vertical lines indicate the instants when we recorded the interferometric frames presented in Figs. 3 and 4. **b** Time-resolved HXR and fusion neutron signals recorded downstream (blue), side-on (green) and upstream (red), at distances of 7 m from the pinch

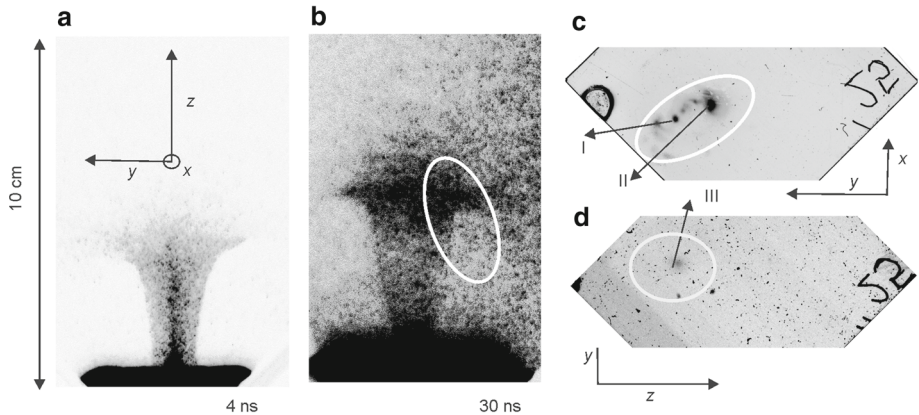


Fig. 3 Data from shot #12760: XUV frames recorded at different instants: **a** during the SXR peak, **b** during the neutron pulse. The deuteron images: **c** from the axial camera, **d** from the slide camera. The intense black spots (with sharp boundaries) were the dust particles, as checked by means of a microscope. The regions of a few spots of deuteron tracks in Figs. 3c and 3d (marked by white ellipses) were up to 3 cm in length. The z -axis corresponded to the anode symmetry axis, while the x - and y -axes were in the plane perpendicular to the z -axis (the x -axis was horizontal, and the y -axis was vertical one)

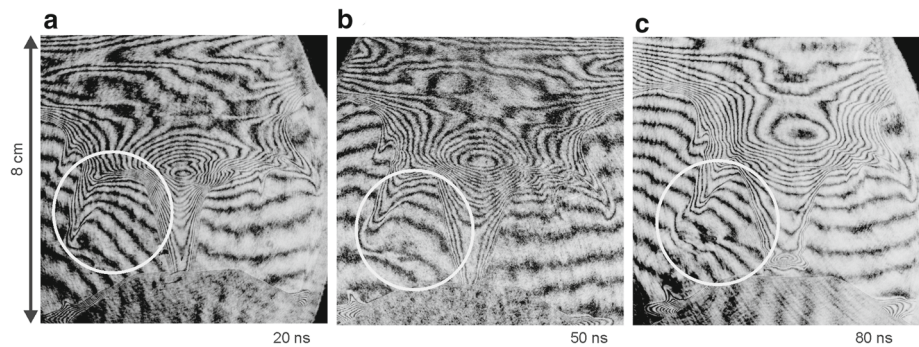


Fig. 4 Other data from shot #12760: the interferometric frames recorded at different instants: **a** at the beginning of the HXR and neutron pulses, **b** at the maximum of the fusion neutron emission, and **c** at the end of the neutron production. All the frames were obtained during the decay of the first plasmoid, which was observed in a form of the dense closed interferometric fringes. The white circles mark the probable localization of the fast deuteron sources in the plasma lobule region

the energy of deuterons producing fusion neutrons (observed in the downstream direction). Then, the energy value of deuterons produced later decreases gradually. This regularity shows a temporal interconnection of sources of the fast deuterons observed in the PF-1000 shots. A mean energy of deuterons moving in the downstream direction could be estimated from a temporal shift of the neutron peaks measured in the downstream and upstream directions. In the considered shot the time-shift of these peaks amounted to 40 ns, and it could be caused by the mean deuteron energies equal to about 70 keV.

The FWHM values of the neutron pulses (shown in Fig. 2) were not considerably larger than those of the HXR, taking into account some broadening (20–30 ns) caused by the neutron energy spectrum measured at a distance of 7 m. It supports a hypothesis about almost simultaneous production of the fast electrons and deuterons (with uncertainty of a few

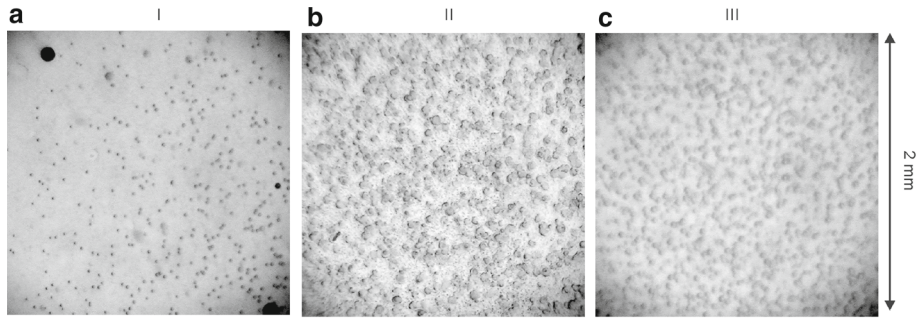


Fig. 5 Microscopic pictures of the deuteron tracks recorded in shot #12760 by means of the axial pinhole camera: **a** the central part of the small spot composed of tracks produced by the fast deuterons, **b** the central part of a bigger spot produced by slower deuterons, and **c** the enlarged image of the spot recorded by the slant camera

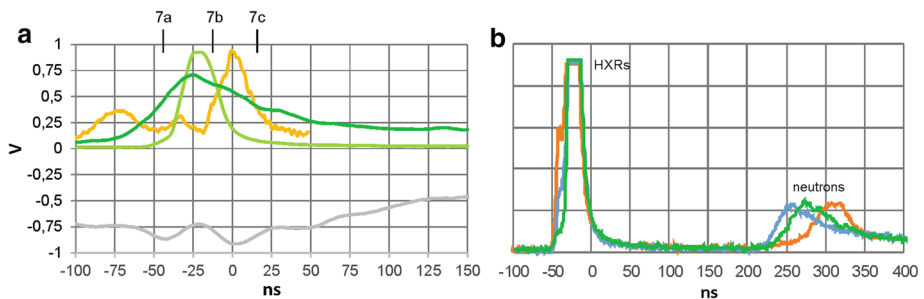


Fig. 6 Data from shot #12759: **a** Waveforms of the current derivative (gray), SXR (yellow), HXR (light green), and fusion-produced neutrons (dark green), recorded side-on and shifted back using the time-of-flight method for neutrons of an averaged energy equal to 2.45 MeV; **b** signals produced by HXR and fusion neutrons, which were recorded downstream (blue), side-on (green) and upstream (red), at distances of 7 m from the pinch

nanoseconds). It should be noted that energy distributions of the considered emissions were very similar, and their energy maximum amounted to about (100–200) keV [38]. The intensity of the recorded HXR signals was reduced due to the absorption of photons of energies below 100 keV in the experimental chamber wall, which is of importance for considerations presented in this paper.

Other experimental data from shot #12760 are presented in Fig. 3.

Figure 3a presents the XUV frame recorded during the first peak of SXR, when the most intense radiation was emitted from the z -axis region. That emission corresponded to the instant of the radial implosion stopping at the minimal diameter of the pinch column. Figure 3b presents another XUV frame, as recorded during the emission of HXR and neutrons. It shows more intense radiation emitted from the first plasmoid and its surrounding (visible in interferometric images presented in Fig. 4a, b in a form of the dense closed interferometric fringes). The production of the fast deuterons temporally corresponded to ongoing decays: (i) of the first plasmoid at the top of the pinch column, (ii) of the pinch constriction, and (iii) of the secondary plasmoids (formed near the anode end). The first plasmoid (during its evolution) absorbed plasma expelled from the neighboring area of the pinch column. Its relatively long lifetime (a few tens of nanoseconds) was apparently caused by a quasi-equilibrium of toroidal and poloidal magnetic field components. The secondary plasmoids were formed during the

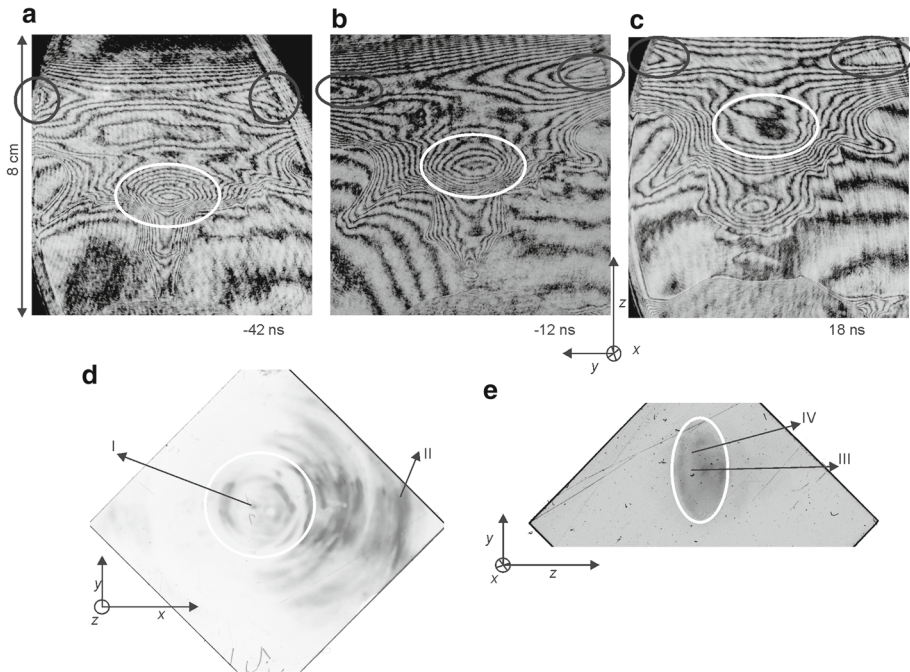


Fig. 7 Data from shot #12759: three interferometric frames recorded during the fusion neutron emission: **a** at the beginning of the HXR and neutron pulses, **b** during HXR and neutron pulses, **c** at the tail of neutron production. The tracks of the fast deuterons were recorded along the z -axis (**d**) and at the angle of 60° (**e**). These tracks are not sharp and circular ones, because the deuteron trajectories were slightly deflected by the external global magnetic fields. The white ellipses show the region occupied by the first plasmoid, and the black ones mark the toroidal plasma structure placed above the current sheath. Its possible current can produce the azimuthal shift in the axial detector. The Roman numbers indicate places imaged by means of an optical microscope

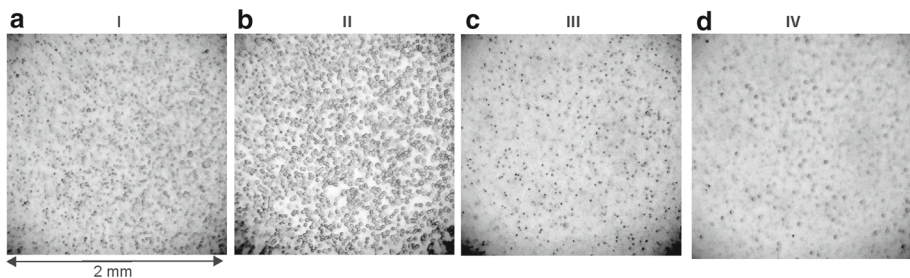


Fig. 8 Microscopic pictures of the deuteron tracks from shot #12759: **a** from the center of the image recorded by the axial camera, **b** from the boundary of that image, **c** from the center of the image recorded by the slant camera, **d** from the boundary of that image, as indicated by the Roman numbers in Fig. 7d, e, respectively. Dimensions of the analyzed tracks show that the recorded deuterons were more energetic than those shown in Fig. 5

final phase of the pinch constriction (along its body). Their lifetime was shorter (up to ten nanoseconds), and they decayed together with the interruption of the pinch constriction.

Hence, it was deduced that the considered processes were associated with the destruction of the closed currents and their magnetic fields, which could be formed also outside of the dense pinch column [26].

Figure 3c, d presents the images of a few spots of deuterons recorded by the axial and slant cameras, respectively. The spots recorded by the axial detector show four important features: (i) the circular symmetry and millimeter dimensions of the individual spots recorded both by the axial and side-on camera, (ii) a weak influence of the global magnetic field on trajectories of the fast deuterons (because after their acceleration this field does not change the spots symmetry and dimensions considerably), (iii) the localization of the deuteron sources (in a radial strip-like region of a plasma lobule surrounding the first plasmoid), and (iv) the possibility of an estimation of the number of the deuterons recorded in each spot.

The main observations can be summarized as follows:

- (i) The small spots of the circular symmetry and (1–3) mm in diameters show that the recorded deuterons were emitted mostly from tiny (probably submillimeter) regions, into a small solid angle, in the agreement with the observations presented in a paper [4].
- (ii) The global magnetic field had evidently a weak influence on the motion of the faster deuterons after their initial acceleration, as one can conclude from the circular symmetry and small dimensions of the recorded track spots.
- (iii) In the reported experiments, the uncertainty in determination of the given dimensions was decreased, in comparison with the results presented in earlier papers [27, 28], to the dimension of the spots ranging to about one millimeter.

Other conclusions can be made also on the basis the interferometric frames from the considered shot, which are presented in Fig. 4.

The axial pinhole camera was oriented along the z -axis, while the observation axis of the slant camera was directed toward the plasma region located at a distance 6 cm in front of the anode plate. The several millimeters uncertainty of the camera position was estimated from the observed deflection of the long rod supporting the camera. The deuteron tracks recorded with the axial camera formed the spots distributed inside one radial strip-like region of the dense plasma column at the same azimuth. The taken measurements made it possible to deduce that the sources of the fast deuterons were probably located in the plasma lobule surrounding of the first plasmoid (marked by white circles in Fig. 4), as it was conjectured in our previous papers [26, 27]. It should be mentioned that this plasma region corresponded to the lobule containing countercurrents, as described in a paper [28].

The track spots presented in Figs. 3c and 3d, which are marked by the Roman numbers, have been analyzed by means of an optical microscope, as shown in Fig. 5.

Figure 5a presents the enlarged image of tracks from a small spot produced by fast deuterons of energy above 150 keV, which was marked as I in Fig. 3c. The enlargements of bigger spots, marked as II and III in Fig. 3c, d, are shown in Fig. 5b, c, respectively. They contained also many tracks formed by the deuterons of lower energies.

The density of the deuteron tracks in the recorded spots decreased from their centers toward boundaries (preserving the circular symmetry). The surface density of the deuterons in the spot was estimated to be about $30,000 \text{ mm}^{-2}$. In the more intense spots there were observed even about 300,000 tracks produced by the deuterons, which penetrated through of a pinhole of $200 \mu\text{m}$ in diameter. In Fig. 3c one can identify about ten deuteron sources. Hence, in the solid angle of steradian one might observe even about 10^7 spots. One can also estimate the total number of the fast deuterons emitted from the considered discharge. From the measured neutron yield equal to 5×10^{10} , the known cross section of D–D reactions equal to about $3 \times 10^{-30} \text{ m}^{-2}$, at the mean deuteron energy of about 100 keV, and the plasma-target surface density equal to 10^{23} m^{-2} , the total number of the emitted deuterons could reach

about 10^{16} . This rough estimation shows that in the reported experiment (using the described pinhole cameras), we recorded a very small fraction of the emitted deuterons only.

A blurred track spot recorded by the slant camera (shown in Fig. 3d) corresponded probably to the deuteron source formed in the region of the first plasmoid and its surrounding. In that case the trajectories of the deuterons were evidently influenced by the magnetic field in radial region of the dense column, similar as described in a paper [27].

As it mentioned above, another interesting discharge was realized during shot #12759. It was a good shot, and it produced the total neutron yield equal to 5×10^{10} . The most important waveforms from this shot are shown in Fig. 6.

The waveforms presented in Fig. 6b show that the amplitudes of HXR were considerably higher than those of neutrons, in a contrary to shot #12760 discussed previously. In this case the neutron energy had a similar character, as in Fig. 2b. It was increasing during the rise of the neutron pulse and decreasing during its decrease. It corresponded to the initial increase and later decrease in the downstream velocity of the fast deuterons, which produced the fusion neutrons. In the considered shot the neutron peaks, as recorded in the downstream and upstream directions (see Fig. 6b), were shifted by about 70 ns. It could be explained by deuterons energies reaching about 150 keV in the downstream direction, i.e., considerably higher than those observed in the shot #12760.

Other experimental data from shot #12759, i.e., some interferometric frames and ion pinhole images, are presented in Fig. 7.

Considering the frames shown in Fig. 7, which were recorded during a decay of HXR and neutron pulses, one can notice that these processes were correlated with the visible decay of the pinch constriction and the secondary plasmoid (near the bottom end) as well as with the decay of the first plasmoid (marked by the white ellipse in the upper part of the dense plasma column). The mass of the decayed first plasmoid was partially confined in its side-on and bottom boundary and partially transported along the z -axis as an explosion of the plasma bubble.

It should be noted that the ion image recorded by the axial pinhole camera (see Fig. 7d) was composed of some concentric azimuthal arcades with the center in the z -axis, similar as in many other PF and Z-pinch experiments, e.g., described in papers [4, 13, 20, 22]. The ring-shape spots are more intense within the same circular slice at the angle of about 120° .

The ring-shaped spots have the radial width of about (1–2) mm and relatively sharp radial boundaries. This dimension corresponds to the uncertainty of measurements with the pinhole camera at the small radial deflection caused by the weak global azimuthal magnetic field. On the contrary, the arc-length of the ring-shaped spots (4–20) mm is caused by a few separated spots (each slightly blurred). This azimuthal blurring can be explained by an influence of the global poloidal magnetic field, which could slightly shift trajectories of the recorded deuterons in dependence on their energies [26, 27]. Hence, one can conclude that the poloidal component of the global magnetic field, during the period of the neutron production, had a stronger influence on the deuteron path than the azimuthal one.

It should here be noted that the majority of the recorded deuteron tracks (above 90%) was distributed outside the projection of the dense plasma column (of about 3 cm in diameter). The recorded deuterons originated probably from the region of the observed plasma lobule and a part of the umbrella-shaped current sheath, as it was concluded in our earlier paper [26]. It suggests that the acceleration of a part of the deuterons population took place in the region, which was outside the viewing field of the laser interferometer. The total number of the track spots (about 50) recorded by the axial camera in the shot #12759 was about one order of magnitude higher than that observed in the shot #12760. The observed distribution of the deuteron sources indicated their azimuthal interconnection.

It was a surprise that a relatively low number of the deuteron spots was recorded near the z -axis of the discharge (see Fig. 7d), where deflections of the deuterons by the azimuthal magnetic field should be very low (due to symmetry and small value of the axial current). This fact suggests that the near axis region of the pinch column could be a very weak source of the fast deuterons in spite of the appearance of the disruption of the constriction and the formation of secondary plasmoids.

Similar as in the shot #12760, the deuteron images from shot #12759 were also analyzed with the optical microscope, and the obtained pictures are presented in Fig. 8.

The distribution of the ring-shaped track spots (with some azimuthal blur) suggests two important features: an azimuthal coherence of the deuteron sources and an influence of the global poloidal magnetic field (also in the region of the radius larger than the dense pinch column). This region corresponded evidently to the exploding plasma bubble, formed during the disruption of the pinch constriction, i.e., during a decay of the plasma column, as observed in various PF experiments [31, 38]. The formation of this bubble started almost simultaneously with the decay of the first plasmoid and the constriction. (An example can be seen in Fig. 7c.) Another phenomenon corresponding with the considered bubble might be the formation of a compact plasma object, as described in a paper [39]. Such a structure was in fact ejected from the dense pinch column in some PF-1000 experiments, and it was observed at distance of about 40 cm in front of the anode end. The measurements taken with axial magnetic probes showed that the described structure had a spherical form and some internal closed poloidal current, which was flowing upon its surface. That compact plasma object was an example of the ordered plasma structure similar to plasmoid, which is formed by the internal closed currents.

As it was mentioned in the description of Fig. 7, the black ellipses marked the side-on projections of the toroidal plasma structure placed above the umbrella-shaped current sheath, where some closed currents could flow and produce the corresponding poloidal magnetic field blurring azimuthally the trajectories of deuterons producing ring-like spots.

The narrow ring-shaped track spots recorded in Fig. 7d outside of the projection of the pinch column correspond probably to some thin azimuthal plasma layers, where the counter-currents could also occur, as described in a paper [27]. Then, the fast deuterons could be accelerated in these layers during a decay of the opposite magnetic fluxes connected with the magnetic reconnection phenomena (also outside the viewing field of the laser interferometer).

The deuteron tracks recorded by the slant camera, and shown in Fig. 7e, formed a few bigger spots. Their blurring was probably caused by some shift of the deuteron trajectories due to an influence of the external magnetic fields.

The spots of fast deuterons, which had a regular azimuthal distribution, were probably associated with the more symmetrical distribution of the discharge current in the pinch column and its surrounding. This distribution, as well as some azimuthal and radial regularity, could be related to the filamentary structures which had the radial and azimuthal components observed experimentally in papers [30, 32, 33].

The noticeable differences in tracks of the fast deuterons recorded in the both discussed shots, i.e., a few randomly distributed micro-spots in shot #12760 and the symmetric ring-shaped spots with some azimuthal blurring in shot #12759, can be explained as follows:

One reason of these differences might be different mean energies of the accelerated deuterons and those of the fusion-produced neutrons, which could be deduced from the temporal positions of the neutron signal maximum recorded by means of the downstream and upstream detectors. The mean energy of the deuterons producing neutrons in shot #12760, equal to about 70 keV, was noticeably lower than 150 keV, estimated for shot #12759. This reason was also manifested by a different amplitude ratio of the HXRs and neutrons pulses.

The lower intensity of the HXRs in shot #12760 could be explained by stronger absorption of the radiation of energy below 100 keV in the chamber wall (assuming the similar energy of accelerated electrons and deuterons in the same shot). Then, the HXRs produced in shot #12759 could undergo a weaker absorption, and they could show a higher ratio of the HXR and neutron amplitudes.

The second difference is indicated by the ring-like configuration of the deuteron tracks and azimuthal blurring of the recorded spots. In a paper [4] there were described some important characteristics of the fast deuterons of a MeV energy range, i.e., submillimeter dimensions of their sources and their emission into a small solid angle leading to the ring-shape configuration of the recorded tracks. The considered high-energy deuterons are not deflected considerably by external magnetic fields. The deuterons of lower energy (e.g. about hundred keV), which produce the dominant part of the fusion neutrons, can be emitted from similar micro-regions, but they can be stronger influenced by the environment [26, 27]. The spots recorded in shot #12760, which had a diameter of a few mm, could be a consequence of the deuteron deflections and some radial shifts of their trajectories in relation to their initial directions. Hence, the radius of the spot could be increased with a decrease in deuteron energy, and the increased diameter of the recorded spots could be caused by the penetration of a deuteron beam through some ordered plasma structures with opposite poloidal currents. In the considered shot, the poloidal magnetic field (associated with a toroidal current) producing the azimuthal blurring was considerably lower. Such a poloidal field might be a reason for an azimuthal shift of the deuterons recorded in the rings. Then, the azimuthal blurring observed in shot #12759 could be caused by a toroidal current flowing in the top of the dense plasma column. Its magnetic field might be a few times stronger than that causing the radial blurring (due to a magnetic field associated with the poloidal current component). The observed small radial blurring shows that the deuterons producing the recorded ring-shaped images were not deflected considerably. They originated probably from some small sources formed inside the ring-shape regions of a diameter even larger than the pinch column. A similar radial blurring (of a millimeter range) could also be observed in the track spots recorded for shot #12760. The small spots produced by the deuterons of energy above 100 keV, which were recorded in the axial direction without any azimuthal blurring, show that in that case the poloidal magnetic field was evidently weaker, similar as its source—the azimuthal current.

Hence, one can conclude that the toroidal structures formed by internal current and the associated poloidal magnetic field play an important role as during the acceleration of the fast deuterons as during their subsequent motion.

In the reported series of PF-1000 discharges, an interesting phenomenon was observed in shot #12746, when a short burst of SXR (with the FWHM equal to 5 ns) from a single “ball-like” plasma structure was recorded, as presented in Fig. 9.

As shown in Fig. 9a, the considered SXR burst was recorded by means of a PIN-type detector shielded with a 10- μ m-thick Be-filter, during the late phase of the observed discharge (at $t = 680$ ns after the dip of the current derivative). The image presented in Fig. 9b was obtained by means of a time-integrating SXR pinhole camera equipped also with the 10- μ m-thick Be-filter. One can see that the “ball-like” plasma structure of about 3 mm in diameter had relatively sharp and regular boundaries, and it emitted more intense SXRs. It is probable that this plasma structure was responsible for this SXR burst.

For shot #12746 there were also recorded several interferometric frames which showed the evolution of the pinch column, but unfortunately in instants before the SXR burst. In order to show a regular tendency of the considered phenomenon, we have chosen an interferometric frame from another shot (see Fig. 9c), recorded in the later phase (at $t = 380$ ns). This frame showed a quasi-spherical plasmoid formed at the top of the pinch column. That

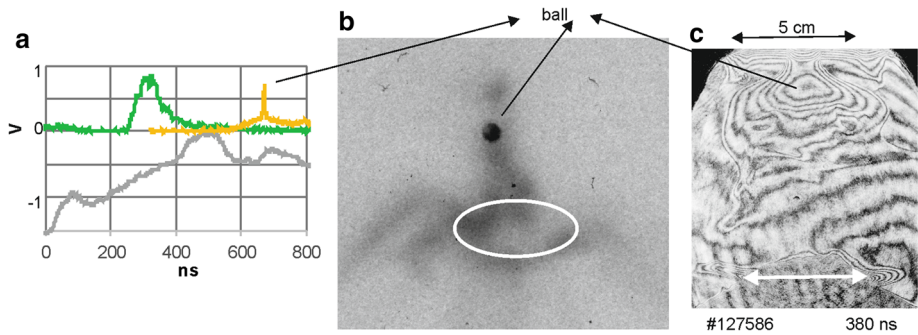


Fig. 9 Data from shot #12746: **a** Waveforms of the current derivative (gray), SXRs signal with a narrow and sharp peak (yellow), and the fusion-produced neutrons recorded side-on (dark green); **b** time-integrated soft X-ray picture of the pinched phase with a radiating “ball-like” structure observed at the angle of 70° to the z -axis. The scale in **b** is the same as shown above **c**. A smaller axial length of the recorded pinch was evidently caused by the chosen observation angle. For a comparison: **c** The interferometric image recorded in the late phase of another shot, which presents the self-generation of a compact plasma structure containing higher internal energy in the late phase of the discharge

plasmoid should contain an admixture of copper ions which were evaporated from the anode surface during the discharge development (at this late phase). The presence of the copper ions in plasma can also be suspected from the interferometer frames, because of the visible irregularities in the interferometric fringes. In any case, the described interferometric frame makes possible to show the formation of some plasma organized structures, e.g., in a form of the regular plasmoids, in a later phase of the discharge. The short intense X-ray pulses are often observed in Z-pinches at the presence of ions of higher z -elements, as so-called “hot spots” [4]. Such emission of the H- and He-like copper lines might be another example of a release of the internal magnetic energy from ordered structures, e.g., through nonthermal radiation.

The probability of the formation of a compact plasma “ball,” radiating in a keV range in PF discharges, seems to be rather very small. We recorded its formation only in one shot during the whole experimental campaign (embracing about hundreds shots). It should, however, be mentioned that a “ball-like” plasma structure of dimensions ranging several mm and lower temperature, which radiated in the XUV range and occupied a quasi-stable position in the plasma column for a relatively long time, was observed regularly in the PF-1000 discharges performed with small amounts of heavier admixtures, as described in a paper [19]. Such structures can be treated as other examples of the ordered magnetic plasma structures formed by some closed internal currents.

4 Summary and conclusions

The main conclusions from the experiments reported in this paper can be summarized as follows:

1. The characteristic waveforms, time-resolved XUV pictures of a dense pinch column, the chosen interferometric frames and time-integrated ion pinhole images, and particularly—the recorded small spots of deuteron-produced tracks, deepened our knowledge about phenomena connected with the production of the fast deuterons.

2. The small (submillimeter) spots of the tracks produced by the fast deuterons from the PF discharges, which have the cylindrical symmetry, show small shifts of the deuteron trajectories in the external magnetic fields. It makes possible to estimate that the sources of the fast deuteron emission have also small (submillimeter) dimensions and small angular dispersion.
3. The deuteron sources are probably located in the region of the dominant plasmoid (formed inside the dense pinch column), as well as in the region of plasma lobules surrounding this column, and possibly in some regions located farther from the z -axis.
4. These regions correspond to the plasma layers in which some countercurrents can flow. They probably decay during magnetic reconnections. Rapid changes of the magnetic fields can induce strong local electric fields, which can effectively accelerate electrons and ions. The fast deuterons (after their axial acceleration) move through the region between two opposite-directed currents, where a weak azimuthal magnetic field can cause a small radial shift only.
5. The recorded group of small deuteron track spots shows some temporal, spatial, and spectral interconnection of different deuteron sources. It is confirmed by their azimuthal and/or radial configuration, formed during a decay of the ordered plasma structures which have cm-range dimensions. It is confirmed also by an evolution of energy of the accelerated deuterons, which increases usually before the peak of the neutron-produced signal, and decreases in later phases.
6. The observed small (mm-range) dimensions, high energy densities, as well as azimuthal and radial configurations of the fast deuteron sources—are probably associated with the filamentary structure of the current flowing in the toroidal and poloidal directions, both in the internal and external regions of the dense pinch column. Such small sources correspond with the idea of the appearance of high-energy density “nodules,” as described in a paper [25]. A small solid angle of the fast deuterons emission confirms the possibility of the ordered plasmoid-like structures.
7. The azimuthal blurring of the ring-shaped deuteron spots can be explained by an influence of the poloidal magnetic field, which acted mainly in the umbrella-shaped current sheath. It might be associated with some toroidal current, which could flow inside the toroidal plasma structure. In this region there was observed a plasma bubble exploding during the disruption of the dense plasma column in all observed PF discharges. The blurring of the deuteron tracks recorded by the slant camera can be explained by an influence of stronger magnetic fields appearing in the radial surrounding of the plasma column.
8. The noticeable differences in the tracks of the fast deuterons recorded in the both discussed shots, i.e., a few randomly distributed micro-spots in shot #12760 and the symmetric ring-shaped spots in shot #12759, can be explained by different intensities of an internal toroidal current and the corresponding poloidal magnetic field. This magnetic field can evidently influence the energy of the accelerated charged particles and the deflections of their trajectories. Unfortunately, we have not enough experimental data to analyze deeper an influence of the poloidal magnetic fields on the acceleration of electrons and ions.
9. The distinct a few nanoseconds lasting peak of the X-ray emission from the observed “ball-like” structure confirmed the appearance of the organized plasma structure of a high energy density. Energy from this structure could be released in a form of a nonthermal burst of keV photons, in analogy to the X-ray emission of higher- z ions from so-called “hot spots.”

In the final conclusion, it should be noticed that the presented results and considerations are qualitative ones. They provide, however, more information about the complexity of the

deuteron acceleration processes. It needs farther experimental, theoretical, and numerical studies—supported by discussions concerning possible interpretation of the collected experimental results in different fusion and astrophysical plasmas. It should be mentioned that such discussions (of results obtained with different PF devices) take place during the annual ICDMP meetings [40].

Acknowledgements This study was supported in part by Research Programs under Grants MSMT LTT17015, LTAUSA17084, CZ.02.1.01/0.0/0.0/16_019/0000778, GACR 19-02545S, IAEA CRP 23071 and 23225, and SGS 16/223/OHK3/3T/13, as well by the Polish Ministry of Science and Higher Education within a framework of the financial resources allocated in 2020 for the realization of the international co-financed projects. The authors wish to express thanks to Mr. Krzysztof Gataarczyk for processing of the nuclear detectors. One of co-authors (M. Akeł) would like to express his thanks to a Director General of AECs for his encouragement and permanent support, as well as to PF-1000 Lab. & ICDMP for some financial support. The raw data were collected at the PF-1000 large-scale facility. The data, supporting the findings of this study, are available from the corresponding author upon a request.

Data Availability Statement This manuscript has associated data in a data repository. [Authors' comment: The data, supporting the findings of this study, are available from the corresponding author upon a request].

References

1. M. Yamada, R. Kulsrud, H. Ji, *Rev. Modern Phys.* **82**, 603 (2010)
2. P.M. Nilson, L. Willingale, M.C. Kaluza, C. Kamperidis, S. Minardi, M.S. Wei, P. Fernandes, M. Notley, S. Bandyopadhyay, M. Sherlock, R.J. Kingham, M. Tatarakis, Z. Najmudin, W. Rozmus, R.G. Evans, M.G. Haines, A.E. Dangor, K. Krushelnick, *Phys. Rev. Lett.* **97**, 255001 (2006)
3. T. Pisarczyk, S. Yu. Guskov, T. Chodukowski, R. Dudzak, P. Korneev, N.N. Demchenko, Z. Kalinowska, J. Dostal, A. Zaras-Szydłowska, S. Borodziuk, L. Juha, J. Cikhardt, J. Krasa, D. Klir, B. Cikhardtova, P. Kubes, E. Krousky, M. Krus, J. Ullschmied, K. Jungwirth, J. Hrebicek, T. Medrik, J. Golasowski, M. Pfeifer, O. Renner, S. Singh, S. Kar, H. Ahmed, J. Skala, P. Pisarczyk, *Phys. Plasmas* **24**, 102711 (2017)
4. A. Bernard, H. Bruzzone, P. Choi, H. Chaqui, V. Gribkov, J. Herrera, K. Hirano, A. Krejci, S. Lee, C. Luo, F. Mezzetti, M. Sadowski, H. Schmidt, K. Ware, C.S. Wong, V. Zoita, *J. Moscow Phys. Soc.* **8**, 93 (1998)
5. L. Bertalot, H. Herold, U. Jager, A. Mozer, T. Oppenlander, M. Sadowski, H. Schmidt, *Phys. Lett.* **79A**, 389 (1980)
6. A. Mozer, M. Sadowski, H. Herold, H. Schmidt, *J. Appl. Phys.* **53**, 2959 (1982)
7. M.G. Haines, *Plasma Phys. Control. Fusion* **53**, 093001 (2011)
8. D.D. Ryutov, M.S. Derzon, M.K. Matzen, *Rev. Mod. Phys.* **72**, 167 (2000)
9. D.D. Ryutov, *IEEE Trans. Plasma Sci.* **43**, 2363 (2015)
10. L. Soto, *Plasma Phys. Control. Fusion* **47**, A361 (2005)
11. V. Krauz, *Plasma Phys. Control. Fusion* **48**, B221 (2006)
12. M. Krisnan, *IEEE Trans. Plasma Sci.* **40**, 3189 (2012)
13. D. Klir, A.V. Shishlov, V.A. Kokshenev, P. Kubes, K. Rezac, R.H. Cherdizov, J. Cikhardt, B. Cikhardtova, G.N. Dudkin, F.I. Fursov, T. Hyblik, J. Kaufman, B.M. Kovalchuk, J. Krasa, J. Kravarik, N.E. Kurmaev, AYu. Labetsky, V. Munzar, H. Orcikova, V.N. Padalko, N.A. Ratakhin, O. Sila, J. Stodulka, K. Turek, V.A. Varlachev, R. Wagner, *New J. Phys.* **20**, 53064 (2018)
14. M. Scholz, L. Karpinski, M. Paduch, K. Tomaszewski, R. Miklaszewski, *Nukleonika* **46**, 35 (2001)
15. M.J. Sadowski, M. Scholz, *Nukleonika* **47**, 31 (2002)
16. P. Kubes, D. Klir, J. Kravarik, K. Rezac, J. Kortanek, V. Krauz, K. Mitrofanov, M. Paduch, M. Scholz, T. Pisarczyk, T. Chodukowski, Z. Kalinowska, L. Karpinski, E. Zielinska, *Plasma Phys. Control. Fusion* **55**, 035011 (2013)
17. P. Kubes, M. Paduch, M.J. Sadowski, J. Cikhardt, B. Cikhardtova, D. Klir, J. Kravarik, K. Rezac, V. Munzar, E. Zielinska, E. Składnik-Sadowska, A. Szymaszek, K. Tomaszewski, D. Zaloga, *J. Fusion Energy* **38**, 490–498 (2019)
18. P. Kubes, M. Paduch, J. Cikhardt, J. Kortanek, B. Cikhardtova, K. Rezac, D. Klir, J. Kravarik, E. Zielinska, *Phys. Plasmas* **21**, 122706 (2014)

19. P. Kubes, M. Paduch, J. Cikhardt, B. Cikhardtova, D. Klir, J. Kravarik, K. Rezac, E. Zielinska, M.J. Sadowski, A. Szymaszek, K. Tomaszewski, D. Zaloga, *Phys. Plasmas* **24**, 032706 (2017)
20. P. Kubes, M. Paduch, M.J. Sadowski, J. Cikhardt, B. Cikhardtova, D. Klir, J. Kravarik, V. Munzar, K. Rezac, E. Zielinska, E. Skladnik-Sadowska, A. Szymaszek, K. Tomaszewski, D. Zaloga, *IEEE Trans. Plasma Sci.* **47**, 339 (2019)
21. V. Krauz, K. Mitrofanov, M. Scholz, M. Paduch, L. Karpinski, E. Zielinska, P. Kubes, *Plasma Phys. Control. Fusion* **54**, 025010 (2012)
22. V.I. Krauz, K.N. Mitrofanov, M. Scholz, M. Paduch, P. Kubes, L. Karpinski, E. Zielinska, *EPL* **98**, 45001 (2012)
23. P. Kubes, M. Paduch, M.J. Sadowski, J. Cikhardt, D. Klir, J. Kravarik, R. Kwiatkowski, V. Munzar, K. Rezac, A. Szymaszek, K. Tomaszewski, E. Zielinska, M. Akel, B. Cikhardtova, *Matter Radiat. Extremes* **5**, 046401 (2020)
24. S. Auluck, *Phys. Plasmas* **27**, 022308 (2020)
25. W.H. Bostic, *Int. J. Fusion Energy* **1**, 1 (1977)
26. P. Kubes, M. Paduch, M.J. Sadowski, J. Cikhardt, B. Cikhardtova, D. Klir, J. Kravarik, V. Munzar, K. Rezac, E. Zielinska, E. Skladnik-Sadowska, A. Szymaszek, K. Tomaszewski, D. Zaloga, *Phys. Plasmas* **25**, 012712 (2018)
27. P. Kubes, M. Paduch, M.J. Sadowski, J. Cikhardt, B. Cikhardtova, D. Klir, J. Kravarik, R. Kwiatkowski, V. Munzar, K. Rezac, E. Skladnik-Sadowska, A. Szymaszek, K. Tomaszewski, D. Zaloga, E. Zielinska, *Phys. Plasmas* **26**, 032702 (2019)
28. P. Kubes, M. Paduch, M.J. Sadowski, J. Cikhardt, B. Cikhardtova, D. Klir, J. Kravarik, R. Kwiatkowski, V. Munzar, K. Rezac, E. Skladnik-Sadowska, A. Szymaszek, K. Tomaszewski, D. Zaloga, E. Zielinska, M. Akel, *Phys. Plasmas* **27**, 092702 (2020)
29. M. Sadowski 1, H. Herold, H. Schmidt, M. Shakhatre *Phys. Letters* **105A**, 117 (1984)
30. M.M. Milanese, O.D. Cortázar, M.O. Barbaglia, R.L. Moroso, *IEEE Trans. Plasma Sci.* **42**, 2606 (2014)
31. L. Soto, C. Pavez, J. Moreno, M.J. Inestrosa-Izurieta, F. Veloso, G. Gutierrez, J. Vergara, A. Clausse, H. Bruzzone, F. Castillo, L.F. Delgado-Aparicio, *Phys. Plasmas* **21**, 122703 (2014)
32. E. Lerner (2020). <https://lppfusion.com/images-catch-ff-2b-in-action/>
33. B.A. Trubnikov, *Plasma Phys. Rep.* **28**, 315 (2002)
34. P. Kubes, M. Paduch, J. Cikhardt, B. Cikhardtova, D. Klir, J. Kravarik, K. Rezac, E. Zielinska, M.J. Sadowski, A. Szymaszek, K. Tomaszewski, D. Zaloga, *Phys. Plasmas* **24**, 092707 (2017)
35. K. Rezac, D. Klir, P. Kubes, J. Kravarik, *Plasma Phys. Control. Fusion* **54**, 105011 (2012)
36. E. Zielinska, M. Paduch, M. Scholz, *Contrib. Plasma Phys.* **51**, 279 (2011)
37. E. Skladnik-Sadowska, K. Czaus, K. Malinowski, M.J. Sadowski, J. Zebrowski, L. Karpinski, M. Paduch, M. Scholz, P. Kubes, I.E. Garkusha, V.I. Tereshin, *Proc. ICDMP-2009 Meeting*, http://www.icdmp.pl/images/2009/skladnik_2009.pdf
38. A. Bernard, A. Coudeville, A. Jolas, J. Launspach, J. de Mascureau, *Phys. Fluids* **18**, 180 (1975)
39. V.I. Krauz, M. Paduch, K. Tomaszewski, K.N. Mitrofanov, A.M. Kharrasov, A. Szymaszek, E. Zielinska, *EPL* **129**, 15003 (2020)
40. www.icdmp.pl.